

Relation between barrier conductance and Coulomb blockade peak splitting for tunnel-coupled quantum dots

John M. Golden and Bertrand I. Halperin

Department of Physics, Harvard University, Cambridge, Massachusetts 02138

(Received 3 May 1995; revised manuscript received 29 October 1995)

We study the relation between the barrier conductance and the Coulomb blockade peak splitting for two electrostatically equivalent dots connected by tunneling channels with bandwidths much larger than the dot charging energies. We find that this problem is equivalent to a well-known single-dot problem and present solutions for the relation between peak splitting and barrier conductance in both the weak- and strong-coupling limits. Results are in good qualitative agreement with the experimental findings of Waugh *et al.*

I. INTRODUCTION

Turning on a tunnel junction to a quantum dot leads to progressive destruction of the single-dot Coulomb blockade.¹ Experiments by Waugh *et al.*² and by Molenkamp, Flensberg, and Kemerink³ chronicle this eradication for two tunnel-coupled dots of equal and widely disparate charging energies, respectively. Inspired by the experimental results of Ref. 2, the present paper seeks to develop a simple model for the coherent tunneling of electrons between a pair of electrostatically identical quantum dots [see Fig. 1(a) for a schematic view of the double-dot structure of Waugh *et al.*]. The goal is to describe the evolution of the Coulomb blockade from that of two isolated dots to that of one composite dot in terms of parameters that determine the states of the isolated dots and the nature of the connection between them. In the limits relevant to the experimental situation in Ref. 2, we find that the most important dimensionless parameters are the number N_{ch} of conducting channels between the two dots and the dimensionless *interdot barrier conductance* g of each channel, which is measured when the Coulomb blockade has been removed. (The interdot barrier conductance was measured in Ref. 2 by de-energizing the external barrier potentials V_{xi} that separate the dots from the leads. This conductance is to be distinguished from the conductance measured in the double-dot Coulomb blockade measurements, which might be referred to as the *Coulomb blockade conductance* or *double-dot conductance*.)

The problem of coupled quantum dots and, more generally, of the effect of tunnel couplings upon the Coulomb blockade has received much attention. Ruzin *et al.*⁴ examined the Coulomb blockade structure of two nonidentical dots in series via a standard activation-energy approach. Stafford and Das Sarma^{5,6} as well as Klimeck, Chen, and Datta⁷ have applied Hubbard-like models with and without interdot capacitances to determine the many-body wave functions for tunnel coupling between a small array of single-dot eigenstates. Many investigators have studied the effect of tunneling upon the Coulomb blockade for metallic junctions, in which there are a large number of conducting channels.⁸⁻¹³ Relatively few have considered junctions with only one or two channels.¹⁴⁻¹⁷ Furthermore, the work on one- or two-channel junctions has been restricted to consid-

eration of a single dot coupled to bulk leads rather than systems of coupled dots. A significant finding of this paper is that by introducing a “fictional” difference between the gate voltages on the individual dots, one can map the two-dot problem onto the one-dot problem and adapt previously obtained results for strong interdot coupling between a single dot and a bulk lead.

In Sec. II of this paper, we present a brief review of the experimental results that have motivated our investigation. In Sec. III A, we define a tunneling model that is useful for calculations in the limit of weak coupling between the two dots. In Sec. III B, we show how a “center-of-mass transformation” allows one to map the two-dot problem onto the one-dot problem. Section IV presents the weak-coupling results for our theory, and Sec. V gives the strong-coupling results and offers plots of the data and theory for one- and two-channel junctions. A summary of our findings is provided in Sec. VI.

II. MOTIVATION

The experiment of Waugh *et al.*² provides the primary motivation for this paper. These authors study the effect that varying the interdot potential barriers has upon the Coulomb blockade conductance peak structure for arrays of n dots, where $n=2$ or 3. For their Coulomb blockade measurements, they energize the confining gates [V_{xi} in Fig. 1(a)] so that the conductance between the dots and the external leads is much less than $2e^2/h$. Having tuned the dots to be electrostatically identical—i.e., to have common gate and total dot capacitances C_g and C_Σ —they find that lowering the interdot barriers results in interpolation between the peak structure characteristic of the isolated individual dots and that characteristic of a single composite dot having capacitance nC_Σ : the initial isolated-dot peaks split into bunches of n subpeaks, and the splitting within the bunched subpeaks increases until they are essentially equally distributed with n times the periodicity of the original peaks [see Figs. 2(b) and 2(c)]. For the double dot ($n=2$), Waugh *et al.* also measure the conductance G_b of the barrier between the two dots after the exterior walls of the double dot have been removed and remark that plots of the subpeak splitting and barrier conductance as functions of the barrier gate voltage appear substantially similar.

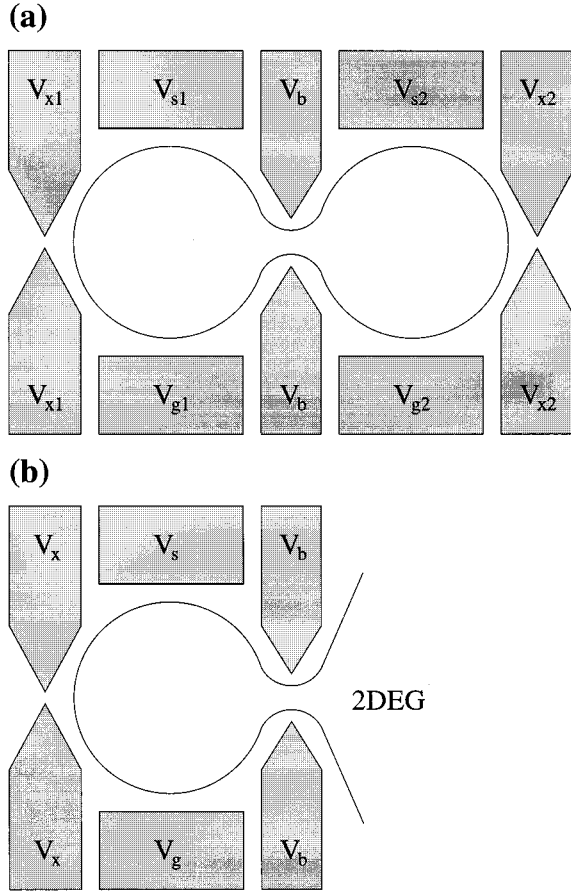


FIG. 1. (a) Schematic diagram for the double dot. Negative potentials are applied to each of the gates to form the double-dot structure. The gate potentials V_{g1} and V_{g2} control the average numbers of electrons on the dots. These are the potentials that are varied to see the Coulomb blockade. V_b controls the rate of tunneling between the dots. V_{x1} and V_{x2} control the rate of tunneling to the adjacent bulk two-dimensional electron gas (2DEG) leads. For calculations of the double-dot energy shifts, tunneling to the leads is assumed negligible compared to tunneling between the two dots. In measuring the barrier conductance G_b , however, the potentials V_{xi} are turned off so that each dot is strongly connected to its lead. The side-wall potentials V_{s1} and V_{s2} are fixed. (b) Schematic diagram for the single dot. V_b now controls tunneling between the dot and the bulk 2DEG. V_g determines the average number of electrons on the dot. For our purposes, V_s and V_x are constant, and tunneling to the bulk 2DEG through the barrier defined by V_x is negligible compared to tunneling through the barrier defined by V_b .

Waugh *et al.* use a $T=0$ “capacitive charging model” to interpret their data. In this model, electrons on the dots are treated as charged particles with no kinetic energy that occupy each dot in integer amounts. In the absence of coupling, the energy is given by the sum of the potential energies of the individual dots. For two dots with common capacitances C_Σ and C_g , the expression for the energy has an especially simple form

$$E = \frac{U}{2} \sum_{i=1}^2 (n_i - \phi_i)^2, \quad (1)$$

where U is the charging energy for each individual dot, $U = e^2/C_\Sigma$; n_i is the number of electrons on the i th dot; and

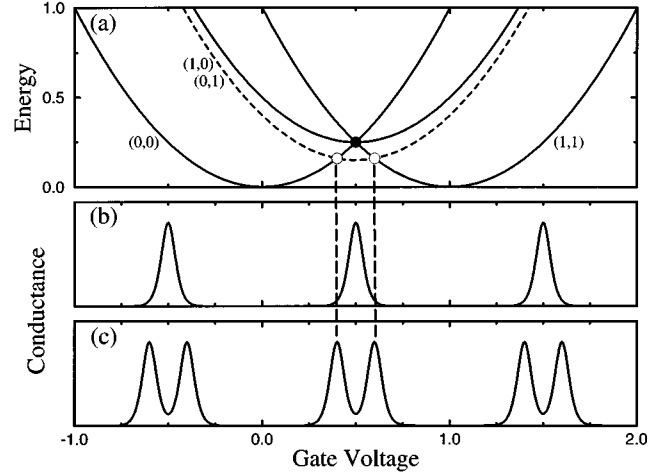


FIG. 2. (a) Energy curves in the capacitive charging model for electrostatically identical dots with $V_{g1} = V_{g2}$ and zero interdot capacitance. Energies are given in units of the charging energy U ; the gate voltage is given in units of e/C_g . Each zero-coupling eigenstate with definite particle number n_i on the i th dot gives rise to a parabola, labeled (n_1, n_2) , which shows the state’s energy as a function of the gate voltage. The zero of energy is chosen to coincide with the lowest energy possible for states with an even value for the total number of particles N_{tot} . The solid odd- N_{tot} parabola gives the lowest-energy curve only when there is no interdot coupling. The dotted parabola is the shifted-down energy curve for odd N_{tot} that results from finite coupling between the dots. The relevant degeneracy points are indicated by a black dot for zero coupling and white dots for finite coupling. (b) “Zero-coupling” conductance through the double dot as a function of the gate voltage. (For ease of viewing, peaks are depicted as symmetric with uniform finite widths and heights.) Conductance peaks are aligned with the zero-coupling degeneracy points such as the one shown in (a) and occur regularly with unit period. (c) Conductance through the dot for finite interdot coupling. Conductance peaks are aligned with the perturbed degeneracy points. Each zero-coupling peak has split into two separate peaks, equally distant from the zero-coupling peak position. Increasing the interdot coupling increases the separation between the paired peaks until the full set of peaks is again regularly distributed, with half the original period. (This figure for the capacitive charging model follows that of Ref. 2.)

ϕ_i is the gate voltage parameter that determines the energy-minimizing value of n_i . For common gate voltages and gate-to-dot capacitances, we have the relations $\phi_i \equiv C_{gi} V_{gi} / e = C_g V_g / e \equiv \phi$. Figure 1(a) should help put these parameters in context.

For each set of integer occupation numbers (n_1, n_2) , the capacitive charging model with $\phi_i = \phi$ gives an energy $E_{(n_1, n_2)}$ that is a parabolic function of the common gate voltage parameter ϕ (see Fig. 2). All the parabolas are identical in shape, their only distinguishing features being the locations of their minima. The lowest-energy parabola $E_{N_{\text{tot}}}(\phi)$ for a given value of $N_{\text{tot}} = \sum_{i=1}^2 n_i$ has $n_1 = n_2 = N_{\text{tot}}/2$ for N_{tot} even and $n_1 = n_2 \pm 1 = (N_{\text{tot}} \pm 1)/2$ for N_{tot} odd. In the former *even* case, the minima all lie on the line $E=0$. In the latter *odd* case, the minima are displaced upward, sitting along $E=U/4$. For all parabolas, the ϕ coordinate of the minimum is $N_{\text{tot}}/2$.

A prominent peak in the double-dot conductance occurs at

values of ϕ such that the lowest-energy parabolas corresponding to consecutive values of N_{tot} cross—in other words, at values of ϕ for which $E_{N_{\text{tot}}}(\phi) = E_{N_{\text{tot}}+1}(\phi)$ for some integer N_{tot} . For the model of Eq. (1), this occurs whenever $\phi = m + \frac{1}{2}$, where m is an integer. (One such crossing point is marked by the black dot in Fig. 2.)

In a model in which coupling between the dots is included, the lowest-energy parabolas for odd N_{tot} are shifted downward relative to the lowest-energy even- N_{tot} parabolas by an “interaction energy” E_{int} . This downward shift splits each of the initial crossing points into a pair of crossing points symmetric about the position of the initial degeneracy, from which they are separated by a distance proportional to E_{int} . As a result, each of the initial conductance peaks is similarly split into two subpeaks with separation proportional to E_{int} . The subpeak splitting reaches its saturation value when $E_{\text{int}} = U/4$ —i.e., when the lowest-energy *even* and *odd* parabolas have the same minimum energy. At this point, the relevant crossing points occur for $\phi = \frac{1}{2}(m + \frac{1}{2})$. The corresponding conductance peaks are once again equally spaced, but their period is now that characteristic of a single dot with capacitance $2C_{\Sigma}$.

Thus, in the capacitive charging model, the problem of explaining the peak splitting reduces to the problem of describing the shift in the ground-state energy of a double dot containing a fixed total number of particles. Waugh² has shown that introduction of a capacitive coupling C_{int} between the two dots would allow one to obtain a picture in qualitative agreement with the experimental results: as the interdot capacitance goes to infinity, E_{int} converges to $U/4$. However, the magnitude of the interdot coupling necessary to fit the experimental data is much larger than what one would expect from an electrostatic interaction between two adjacent dots having a narrow tunneling channel between them. Waugh *et al.*² found that in order to bring about the saturation peak splitting, the interdot capacitance would have to grow from its zero-tunneling value by approximately a factor of 250, to a magnitude 10 times larger than the single-dot capacitances at zero tunneling. If one were to model the two dots as coplanar sheets of charge being moved closer together as the interdot channel conductance g is increased—essentially a best case scenario for those wishing to induce large interdot capacitances—the intercapacitance would depend only logarithmically on the separation, and the distance between the dots would have to be decreased to much less than an interatomic length to effect the required growth.

Consequently, the use of a large interdot capacitance C_{int} must be regarded as simply a reparametrization of the problem that replaces one unknown, E_{int} , with another unknown, C_{int} . What we really want is a theory that produces agreement with experiment and expresses E_{int} in terms of simple measurable quantities. Waugh *et al.* provide one candidate: the conductance G_b of the barrier between the two dots. The remainder of this paper is devoted to developing a theory of the relation between E_{int} and the dimensionless conductance per tunneling channel $g = G_b/N_{\text{ch}}G_0$, where N_{ch} is the number of independent interdot tunneling channels (assumed to have identical conductances) and G_0 is the conductance quantum e^2/h . In the experiment of Ref. 2, there is no applied magnetic field and the dots are connected by a

narrow constriction allowing only a single transverse orbital mode with double spin degeneracy. As a result, in this experimental case, $N_{\text{ch}} = 2$.

III. TUNNELING MODEL FOR THE DOUBLE-DOT COUPLING

A. Definition of the model

Our goal can be stated a bit more precisely. For a general tunnel coupling between two dots involving any number N_{ch} of identical, independent channels and dimensionless channel conductance g , our aim is to express the fractional energy shift $f \equiv E_{\text{int}}/(U/4)$ as a function of g and N_{ch} plus any other parameters that might be found to be important. In order to derive an equation for f , we first choose a double-dot Hamiltonian. We will ignore electrostatic coupling of the dots for the moment: it will be noted at the beginning of Sec. III B that the presence of an interdot capacitance makes no substantive difference for our analysis. Interaction between the dots will occur solely via tunneling through the barrier between them. Such tunnel Hamiltonians have been found useful from the beginnings of Coulomb blockade theory,¹⁸ and the model we will use is a double-dot version of the Hamiltonian used, for example, by Averin and Likharev to investigate the conductance oscillations of small metal-to-metal tunnel junctions.¹⁹ In particular, we have the Hamiltonian $H = H_0 + H_T$, where

$$H_0 = K + V,$$

$$K = \sum_{i=1}^2 \sum_{\sigma} \sum_{\mathbf{k}} \epsilon_{i\mathbf{k}\sigma} \hat{n}_{i\mathbf{k}\sigma},$$

$$V = \frac{U}{2} \sum_{i=1}^2 (\hat{n}_i - \phi_i)^2,$$

$$H_T = \sum_{\sigma} \sum_{\mathbf{k}_1 \mathbf{k}_2} (t_{\mathbf{k}_1 \mathbf{k}_2} c_{2\mathbf{k}_2 \sigma}^{\dagger} c_{1\mathbf{k}_1 \sigma} + \text{H.c.}). \quad (2)$$

In these equations, i is the dot index, σ is the channel index (which could signify different spin channels), and \mathbf{k} is the index for all internal degrees of freedom not included in the channel index. In addition, $\hat{n}_i = \sum_{\mathbf{k}\sigma} \hat{n}_{i\mathbf{k}\sigma}$ is the number operator for the i th dot, and $t_{\mathbf{k}_1 \mathbf{k}_2}$ is the tunneling matrix element between a dot 1 wave function indexed by \mathbf{k}_1 and the dot 2 wave function lying in the same channel and indexed by \mathbf{k}_2 . The gate voltage parameter ϕ_i has the same meaning as in Eq. (1). $\epsilon_{i\mathbf{k}\sigma}$ is the kinetic energy of the single-particle eigenstate of the i th dot having the indicated degrees of freedom. For simplicity, we will take these energies to be independent of dot and channel: $\epsilon_{i\mathbf{k}\sigma} = \epsilon_{\mathbf{k}}$.

The next step in focusing upon a model Hamiltonian is to choose a form for $t_{\mathbf{k}_1 \mathbf{k}_2}$. Quite generally, $t_{\mathbf{k}_1 \mathbf{k}_2}$ will be non-zero only when both \mathbf{k}_1 and \mathbf{k}_2 lie within some wave-vector shell that maximally spans the space between the theory's low- and high-momentum cutoffs. The size of the wave-vector shell depends on details of the barrier—in particular, the characteristic lengths of the channel both parallel and perpendicular to the voltage wall between the dots. If the barrier has an abrupt δ -function shape, the tunneling wave-

vector shell will span all of reciprocal space. If, on the other hand, the channel evolves adiabatically from the dots, the shell width will be small on the scale of a Fermi wave-vector. Important questions are how many states lie within this shell—i.e., how large is the width W of the corresponding energy shell compared to the average level spacing δ between different states in the same channel (hereafter referred to as “the average level spacing” or just “the level spacing”)—and, for a given \mathbf{k}_1 , for how many \mathbf{k}_2 is $t_{\mathbf{k}_1\mathbf{k}_2}$ nonzero. Thin-shell models with “one-to-one” hopping elements (i.e., for which $t_{\mathbf{k}_1\mathbf{k}_2}=0$ unless $\mathbf{k}_1=\mathbf{k}_2$) have been applied to the coupled-dot problem with some success,^{5–7} especially for level spacings δ that are on the order of the charging energy U . For the nearly micrometer-sized dots used by Waugh *et al.*,² however, U is approximately 400 μeV and δ is on the order of 30 μeV , so we expect that a tunnel coupling sufficient to destroy the isolated-dot Coulomb blockade will involve a large number of single-dot eigenstates. Indeed, as it does appear that the characteristic size of the channel approximates a Fermi wavelength (40 nm),²⁰ it is reasonable to suppose that the wave-vector shell width is on the order of a Fermi wavevector and, therefore, that the energy shell width W is comparable to the Fermi energy (13 meV), which is much larger than U .

Consequently, assuming an abrupt tunnel barrier, we consider a thick-shell model that is the antithesis of the injective thin-shell model. Working in a regime where $W \gg U \gg \delta$, we use a tunneling matrix element t that is independent of \mathbf{k}_1 and \mathbf{k}_2 within the shell:

$$t_{\mathbf{k}_1\mathbf{k}_2} = t, \quad \forall \mathbf{k}_1, \mathbf{k}_2 \quad \text{such that} \quad \epsilon_0 < \epsilon_{\mathbf{k}_1}, \epsilon_{\mathbf{k}_2} < \epsilon_0 + W.$$

As the quantities we calculate are independent of the phase of t , we guiltlessly choose t to be real. This model is roughly equivalent to one in which each dot is represented by a tight-binding lattice with intersite hopping elements of order W/δ and where interdot tunneling occurs via a tunneling Hamiltonian with a single site-to-site connection. Choosing these tunneling sites to be at the origins $\mathbf{0}_1$ and $\mathbf{0}_2$ of the respective lattices, we may write

$$H_T = \sum_{\sigma} (Tc_{2\mathbf{0}_2\sigma}^\dagger c_{1\mathbf{0}_1\sigma} + \text{H.c.}),$$

where $T \equiv N_W t$ and $N_W = W/\delta$ is the number of orbital states per channel in each dot within the bandwidth W . (The equivalent lattice model should include second- and further neighbor hopping so that the density of states is approximately constant between ϵ_0 and $\epsilon_0 + W$. The lattice constant is chosen by requiring that the product of N_W and the area of a unit cell equals the area of a single dot.)

As the Fermi energy ϵ_F must be somewhere between ϵ_0 and $\epsilon_0 + W$, the meaning of ϵ_0 depends on the width of the band. For a maximally thick shell, ϵ_0 lies at the bottom of the conduction band, and W is an ultraviolet cutoff, which is chosen to be of order twice the Fermi energy. Alternatively, when the barrier between the dots has a broader spatial extent, the energy shell sits more narrowly about the Fermi energy, and the width W is on the order of the energy difference needed to produce a factor-of-2 change in the magni-

tude of the transmission amplitude for an incident particle. We define a dimensionless filling parameter

$$F \equiv \frac{\epsilon_F - \epsilon_0}{W},$$

which gives the position of the Fermi level within the bandwidth W . Provided that $(1-F)W$ and FW are both large compared to U , our final results should be independent of the precise values of W or F .

B. Map between the double- and single-dot systems

The model we have constructed is basically the two-dot version of that used by Glazman and Matveev¹⁴ and Grabert¹³ to study the charge fluctuations of a single metal particle connected via point-tunnel junctions to conducting leads [see Fig. 1(b)]. Indeed, by using an analog of the standard center-of-mass transformation of classical mechanics and fixing the total number of particles in the two-dot system, we can create an exact mapping between the two-dot and one-dot problems. Consider again the double-dot potential energy V . By transforming to the analog of center-of-mass coordinates, one generates the following form:

$$V = \frac{U_1}{4} (\hat{N}_{\text{tot}} - \Phi_{\text{tot}})^2 + U_2 (\hat{n} - \rho/2)^2, \quad (3)$$

where $\hat{N}_{\text{tot}} = \sum_{i=1}^2 \hat{n}_i$, $\Phi_{\text{tot}} = \sum_{i=1}^2 \phi_i$, $\hat{n} = (\hat{n}_2 - \hat{n}_1)/2$, $\rho = \phi_2 - \phi_1$, and $U_1 = U_2 = U = e^2/C_\Sigma$ when the interdot capacitance is zero. The rationale for the normalizations for \hat{n} and ρ will soon be made apparent. In the meantime, note that, for our Hamiltonian, N_{tot} is a constant of motion. Thus, for given N_{tot} , Φ_{tot} , and U_1 , we can drop the first term and insert in the Hamiltonian a reduced potential energy:

$$V_{\text{red}} = U_2 (\hat{n} - \rho/2)^2. \quad (4)$$

The impact of a nonzero interdot capacitance can now be trivially included: its only effect is to decrease the value of U_2 .

In particular, in unpublished work,²¹ Crouch and Golden have found that if C_Σ is defined to be the total capacitance for a single dot minus the interdot capacitance, introduction of a constant interdot capacitance C_{int} decreases U_2 from e^2/C_Σ to $e^2/(C_\Sigma + 2C_{\text{int}})$. The equality $U_1 = U = e^2/C_\Sigma$ is left unchanged. For a given value of the conductance parameter g , if f is the fractional peak splitting in the model with zero capacitive coupling between the dots, then the fractional splitting f' for a system with an interdot capacitance is simply related to f by the equation

$$(1 - f') = \frac{U_2}{U} (1 - f). \quad (5)$$

Capacitive coupling between the dots thus leads to a nonzero splitting ($f' \neq 0$) even when there is no tunneling between the dots ($f = g = 0$).

We can now return to Eqs. (3) and (4). Restrict N_{tot} to be even. Then, \hat{n} has integer expectation values in all the unperturbed double-dot eigenstates. With the total number of particles in the two dots held constant and even, the Hamiltonian is exactly that of a single dot tunnel-coupled to an

ideal lead. The dot has number operator \hat{n} , charging energy $2U_2$, and gate voltage parameter $\rho/2$. In the absence of tunneling and with the level spacing in both dots much less than U_2 , the ground state is an eigenstate of \hat{n} that minimizes the reduced potential energy, which in the future we consider equivalent to “the potential energy.” For $\rho=0$, the minimum potential energy is zero and is achieved when the eigenvalue n of \hat{n} is zero—i.e., when there are equal numbers of particles in the two dots. All other values of n give higher potential energies. For $\rho=1$, on the other hand, the minimum potential energy is $U_2/4$, and $n=0$ and $n=1$ give degenerate minima.

These no-tunneling distinctions between zero and $U_2/4$ and between nondegeneracy and double degeneracy are quite familiar: they characterized the *even* and *odd* double-dot ground states ($\rho=0$ for both) discussed in Sec. II. Indeed, what we called the “*even* double-dot ground state” is precisely the “ N_{tot} even, $\rho=0$ ground state.” The “*odd* double-dot ground state” is not exactly the same as the “ N_{tot} even, $\rho=1$ ground state”; there is no getting around the fact that one case has one more (or less) particle than the other. However, in terms of their ground-state energies, the difference between the two will be down by a factor of FN_W or $(1-F)N_W$. For a wide shell somewhere in the vicinity of half-filling, both FN_W and $(1-F)N_W$ are much greater than 1, and the above difference is negligible. Calculation of E_{int} with $\phi_1 = \phi_2$ for the double dot is therefore equivalent to calculating the relative shifts of the $\rho=0$ and $\rho=1$ ground states of a single dot tunnel-coupled to a bulk two-dimensional electron gas. Having arrived at this conclusion, we will find that we have made much easier the job of solving Waugh’s two-dot problem in the strong coupling regime: we can now redirect earlier work on the one-dot problem to our purpose.

More generally, we observe that we have created a model that extends beyond Waugh’s experiment to circumstances where the two dots have different gate voltage parameters. Such situations can also be mapped to the one-dot problem. As the minimum potential energy is periodic in ρ with period two and is also even in ρ , the general solution is given by that for ρ in the interval $[0,1]$. For ρ in this interval, the difference in the ground-state energies of the double-dot system for even N_{tot} and odd N_{tot} is related to the difference in the ground-state energies of the single-dot system for gate voltage parameters ρ and $1-\rho$. The theory developed in this paper permits calculation of the relative downward shift of the $\rho \neq 0$ ground state to the $\rho=0$ ground state. Dividing by the zero-tunneling energy difference of the two ground states, we find that our emended aim is to calculate

$$f_\rho \equiv \left(\frac{E_{\text{int}}(\rho)}{U_2 \rho^2 / 4} \right) = \Psi_\rho(g, N_{\text{ch}}, u, N_W, F), \quad (6)$$

where $0 < \rho \leq 1$, $u = U_2/W$, $N_W = W/\delta$, and $E_{\text{int}}(\rho)$ is the ground-state energy relative to the ground-state energy for $\rho=0$.

IV. RESULTS IN THE WEAK-COUPLING LIMIT

A. Barrier conductance in the weak-coupling limit

Before we can derive our equation for f_ρ in terms of g , we must find a formula for the barrier conductance. Measure-

ment of the barrier conductance G_b with the exterior gates turned off can be modeled by calculating the tunnel junction conductance for $U_1 = U_2 = 0$. As mentioned before, we assume the different conducting channels to be identical yet independent—their individual conductances are the same and they do not interfere with one another. These assumptions are certainly reasonable for the two spin channels in the experiment of Ref. 2. Using the Lippmann-Schwinger equation with H_T inserted for the scattering potential,²² one can solve for the perturbed electron eigenfunctions. The Heisenberg equation of motion for \hat{n}_1 can then be used to solve for the particle flow from dot 1 to dot 2 for a given voltage bias. Solving the resulting expression for the linear conductance gives the following equation for the dimensionless conductance per channel:

$$g = \frac{G_b}{N_{\text{ch}} G_0} = \frac{4\alpha}{|1 + \chi\alpha|^2}, \quad (7)$$

where $\alpha = (\pi T/W)^2 = (\pi t/\delta)^2$ and

$$\chi = \left[1 + \frac{i}{\pi} \ln \left(\frac{F}{1-F} \right) \right]^2.$$

This equation generalizes Frota and Flensberg’s result for half-filling ($F=0.5, \chi=1$), derived via a Green’s-function–Kubo-formula approach.¹⁵ It is reassuring to note that despite χ ’s imaginary part for $F \neq 0.5$, the maximal dimensionless conductance is one for all filling fractions.

The calculated conductance G_b exhibits rather curious behavior: it first rises to a maximum of $N_{\text{ch}} G_0$ corresponding to N_{ch} fully open channels and then falls asymptotically to zero as $(T/W = t/\delta) \rightarrow \infty$. As Frota and Flensberg note,¹⁵ the asymptotic damping of the conductance results from the fact that formation of bonding and antibonding states at the tunnel junction makes the cost of passing through prohibitively high. The limit of $(T/W = t/\delta) \rightarrow \infty$ is in some sense unphysical: we do not expect a point-to-point hopping coefficient T to significantly exceed the tunneling shell width; nor do we expect the tunneling matrix element t to be much greater than the average level spacing. Nevertheless, the apparent absence of any good reason to truncate the theory at a particular value of t indicates that the model is at best unwieldy in the limit of strong coupling. To get the correct limiting behavior for strong coupling, it is more convenient to use a different approach, suitable for perturbation about the $g=1$ limit. This will be described in Sec. V.

B. Relative energy shift of *even* and *odd* states in the weak-coupling limit

In the meantime, the site-to-site tunneling model is still useful in the weak-coupling regime. So we plod ahead, calculating via standard Rayleigh-Schrödinger perturbation theory the second-order shift in the ground-state energy for $\rho \neq 0$ minus that for $\rho=0$. The $\rho=1$ shift will be taken to equal the limit of the general $0 \leq \rho < 1$ shift as $\rho \rightarrow 1$. It might be objected—correctly—that this limit fails properly to account for the degeneracy of the ground state at $\rho=1$. Such a failing is pardonable, however, for the contributions that are left out are all smaller by a factor of FN_W or $(1-F)N_W$

from those that are retained. Since we assume that t/δ is finite, F is of order $\frac{1}{2}$, and N_W is large, the omitted terms are negligible.

For $N_W \gg 1$, the perturbation-theory sums can be approximated as integrals. Observing that $u \equiv U_2/W \ll 1$, we divide the difference between the second-order shifts by $U_2\rho^2/4$ to get the leading approximation to f_ρ :

$$f_\rho^{(1)} = 4N_{\text{ch}} \frac{t^2}{\delta^2} [(1-\rho)\ln(1-\rho) + (1+\rho)\ln(1+\rho) + O(u\rho^2)]/\rho^2. \quad (8)$$

The second-order term indicates a significant feature of f_ρ : it

is even in ρ . This property has also been noted by Grabert¹³ and results from the fact that at any order of perturbation theory, every tunneling process contributing to the energy shift has a twin with the roles of dots 1 and 2 interchanged. In any intermediate virtual state with eigenvalue n for \hat{n} , the potential energy is greater than that for the unperturbed ground state by $\delta V(\rho) = U_2 n(n-\rho)$. Therefore, when dots 1 and 2 are interchanged, $\delta V(\rho) \rightarrow \delta V(-\rho)$ for all the intermediate states. If we represent one of the twin terms by $\Delta(\rho)$, the other is $\Delta(-\rho)$, and we see that f_ρ is constructed of sums that are even in ρ .

Using the second-order (in t/δ) parts of g and f_ρ , we can now write a first-order equation for f_ρ in terms of g :

$$f_\rho^{(1)} = \frac{N_{\text{ch}}g}{\pi^2} \frac{[(1-\rho)\ln(1-\rho) + (1+\rho)\ln(1+\rho) + O(u\rho^2)]}{\rho^2}, \quad (9)$$

a result consistent with the large- N_{ch} calculation of the effective capacitance of a single dot at $\rho=0$.⁸ Setting $\rho=1$ to calculate the relative shifts of the original *even* and *odd* states, we find

$$f^{(1)} = \frac{2\ln 2}{\pi^2} N_{\text{ch}}g + O(ug, g^2), \quad (10)$$

where we have used the fact that f as originally defined without the subscript is equivalent in our limits to $f_{\rho=1}$. The above equation indicates that the plot of f as a function of gate voltage is not just a replica of the plot for g as a function of gate voltage—as a *prima facie* look at the data of Waugh *et al.* might lead one to suppose.² In particular, for $g \ll 1$ and $N_{\text{ch}}=2$, Eq. (10) gives a slope of approximately 0.28 for $f(g)$, rather than unity. Thus, in this regime, the fractional splitting f of the double-dot conductance peaks should lag g , the dimensionless barrier conductance per channel.

V. CONNECTION TO THE STRONG-COUPPLING LIMIT

If we blithely extended our perturbative equation for f to the limit $g \rightarrow 1$, the large- N_{ch} f would greatly overshoot its mark and the one- or two-channel f would fall substantially short. The real issue is not, however, how badly such a naive extrapolation fails, but whether we can connect these weak-tunneling results to those that can be calculated for the strong-tunneling limit. Having discussed the equivalence of the two-dot and one-dot problems at length in Sec. III B, we can turn to see what the current literature on the one-dot problem offers. For the large- N_{ch} limit, a reasonable interpolation between the solutions for weak and strong coupling has already been found.^{8,9,11}

The situation is less clear for the case with which we are most concerned, in which $N_{\text{ch}}=1$ or 2. Flensberg and Matveev^{16,17} have proposed a useful Luttinger-liquid approach in which the nearly transparent link between a single

dot and an electrode is modeled as a one-dimensional channel with a slightly reflective potential barrier. Convergence to the single composite-dot limit is achieved naturally and neatly, and E_{int} is calculated perturbatively in r , where r is the reflection amplitude, and $g = 1 - |r|^2$. Using the map between the two-dot and one-dot problems, we can translate Matveev's calculations of the leading term for $(1-g) \ll 1$ to our language. We find that for $N_{\text{ch}}=1$ (i.e., assuming spin polarization), the fractional peak splitting in the two-dot problem when $\rho=0$ is given by the following:

$$f = 1 - C_1 \frac{8e^\gamma}{\pi^2} \sqrt{1-g} + \dots, \quad (11)$$

where $\gamma \approx 0.577$ is the Euler-Mascheroni constant and C_1 is an error factor on the order of 1 that we have inserted to guard against the possible imprecision of calculating in Luttinger-liquid theory with a finite cutoff.²³ For the case relevant to the experiment of Ref. 2, $N_{\text{ch}}=2$, adaptation of Matveev's calculation gives

$$f = 1 + C_2 \frac{16e^\gamma}{\pi^3} (1-g)\ln(1-g) + \dots, \quad (12)$$

where C_2 is an error factor analogous to C_1 . Except for the logarithmic factor in the second formula, these equations are of the form suggested by the scaling analysis of Flensberg,¹⁶ which predicts effective charging energies behaving as $(1-g)^{N_{\text{ch}}/2}$. Matveev's initial two-channel solution is, in fact, linear in $(1-g)$ but diverges logarithmically as $U_2/\delta \rightarrow \infty$. A higher-order analysis to eliminate the divergence¹⁷ replaces the logarithm with argument U_2/δ by one with argument $(1-g)^{-1}$.

In Fig. 3, we show the f -versus- g plots given by the weak- and strong-coupling formulas (10), (11), and (12) for $N_{\text{ch}}=1$ and $N_{\text{ch}}=2$ with $C_1=C_2=1$. In each case, a possible interpolation between the weak- and strong-coupling limits is

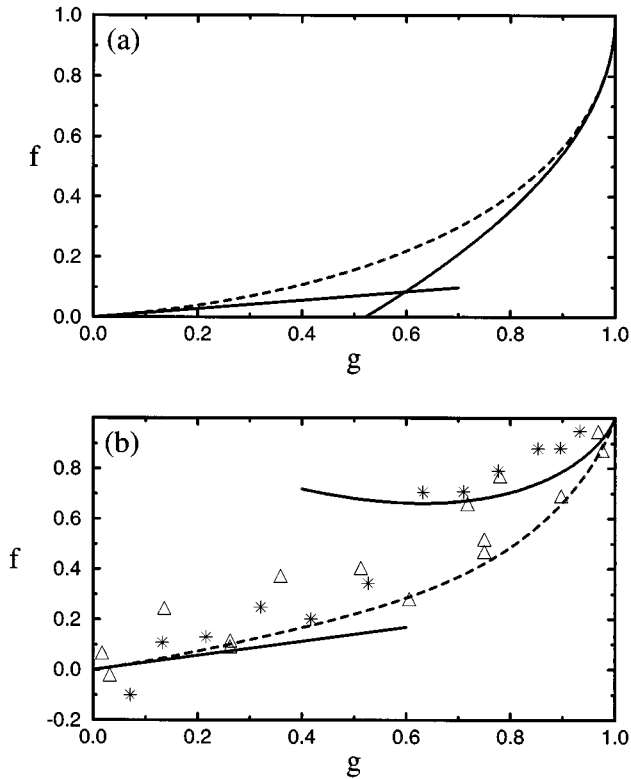


FIG. 3. Graphs of the fractional Coulomb blockade conductance peak splitting f as a function of the dimensionless conductance per channel g in the weak- and strong-tunneling limits for (a) $N_{\text{ch}}=1$ and (b) $N_{\text{ch}}=2$ with coefficients $C_1=C_2=1$ in Eqs. (11) and (12). Possible interpolating functions are shown by dashed curves. Data points from Ref. 2 are given as triangles or stars; the two different symbols correspond to different data sets. The value of f for the experimental data has been extracted from the measured splitting fraction f' as discussed in of Sec. III B with $U_2/U \approx 0.9$. This choice of U_2/U corresponds to the constant interdot capacitance of 20 aF and total single-dot capacitance of 0.4 fF estimated for the experiment of Ref. 2.

given by a dashed curve. For $N_{\text{ch}}=2$, the corresponding experimental data of Waugh *et al.*² are also plotted. Given the experimental error implicit in the dispersion of the data points themselves, the data are seen to be in reasonable agreement with theory.

It is clear, however, that, unlike the calculations for $N_{\text{ch}} \gg 1$, for $N_{\text{ch}}=2$ the order of calculation completed so far does not really allow confident interpolation between the weak- and strong-coupling limits. On the strong-tunneling side, $C_2 \approx 1.5$ would effect greater agreement with our suggested interpolation: Luttinger-liquid theory's prediction of $C_1=C_2=1$ must certainly be checked. With respect to the weak-tunneling results, calculation of higher orders in perturbation theory should improve the matching, but such computations are made difficult by the fact that the correlations induced by the strong Coulomb interaction make normal Green's-functions methods inapplicable.¹² Different time orders must be treated separately, and as appears to occur quite generally in Coulomb-blockade problems,²⁴ the number of diagrams grows pathologically with the order in perturbation theory. Nevertheless, calculation of the g^2 term in the weak-

tunneling limit is conceivable, and this term may permit a more reliable interpolation between the weak- and strong-coupling regimes.

Irrespective of the difficulty of connecting the strong- and weak-coupling limits, it should be emphasized that despite the uncertainty in the coefficients C_1 and C_2 , the strong-coupling results do give an important constraint on the form of the theoretical f -versus- g curves—viz., the value of f must reach 1 at the point where g equals 1. Thus, a model that treats the Coulomb blockade peak splitting as a function of the interdot channel conductance produces the experimentally observed saturation splitting for a reasonable physical value of the parameter g that marks the strength of the interdot coupling. This fact can be understood by noting that a nonzero interdot conductance results in charge fluctuations between the dots for which the natural energy scale is U_2 , the energy scale that characterizes the difference between the $\rho=0$ and $\rho \neq 0$ ground states. As g increases, larger and larger charge fluctuations, in which multiple electrons move from one dot to the other, become increasingly significant, and the initial $g=0$ difference between the $\rho=0$ and $\rho \neq 0$ ground states becomes less relevant to the energy of the $g \neq 0$ ground states, which after all are superpositions of a great number of $g=0$ eigenstates with a wide variety of charge distributions.

The decrease in the ρ dependence of the ground-state energy for $g \neq 0$ could be described, at least approximately, by an “effective interdot capacitance.” However, the introduction of such a fictive and, as noted in Sec. II, unphysical mediator merely begs the question of how such a large effective interaction is produced. Tunneling provides an answer by allowing electrons to hop back and forth between the dots, interacting directly with their “neighbors” through the preexisting $g=0$ two-dot capacitances.

VI. CONCLUSION

Following the work of Waugh *et al.*,² we have investigated the relation between the barrier conductance and the Coulomb blockade for two electrostatically equivalent dots connected by one or more identical tunneling channels and have found an explanation for the evolution of the double-dot Coulomb blockade that does not rely upon unphysically large values for the interdot capacitance, the intradot level spacing, or the number of conducting channels. We propose to write the fractional peak splitting f of the Coulomb blockade conductance peaks as a function of the number of channels N_{ch} and the dimensionless barrier conductance per channel g , assuming that the energy level spacing δ is small compared to the interdot Coulomb blockade energy U_2 and that U_2 is small compared to the bandwidth W of states over which the amplitudes for transmission through the barrier are roughly constant. Using a “uniform thick-shell model” for the tunneling term in the Hamiltonian, we solve for this function to leading order in the limit of weak interdot coupling. We find that in this limit, the peak splitting should evolve linearly with the total barrier conductance with a slope substantially less than 1.

In order to solve for the strong-coupling limit, we have introduced a “fictional” difference between the gate voltages on the individual dots. Such a generalization of the two-dot

problem makes it relatively straightforward to adapt our analysis to situations where there is a voltage bias between the two dots.²⁵ Its purpose here is to allow for a map between the previously unsolved two-dot problem and a better-known one-dot problem. The strong-coupling results that we obtain via this mapping give an asymptotic form for the peak splitting that behaves as $(1-g)\ln(1-g)$.

In the case of $N_{\text{ch}}=2$, which is pertinent to the experimental results of Ref. 2, the present limiting forms for strong and weak coupling do not match up well enough to allow a reliable quantitative interpolation between the two limits. Nevertheless, a plausible interpolating curve is in qualitative agreement with existing experimental data. More precise experimental results would allow for a test of the slope predicted for the weak-tunneling limit. An extension of current

theory is still necessary to permit a convincing connection between the two asymptotic limits.

ACKNOWLEDGMENTS

The authors are grateful for very helpful discussions with F. R. Waugh, R. M. Westervelt, Gergely T. Zimanyi, C. A. Stafford, C. Crouch, C. Livermore, and Steven H. Simon. J.M.G. thanks the United States Air Force for financial support. This work was also supported by the NSF through the Harvard Materials Research Science and Engineering Center, Grant No. DMR94-00396. After this manuscript was essentially complete, the authors received a copy of a paper by Matveev, Glazman, and Baranger prior to publication²⁶ in which similar ideas were independently developed.

-
- ¹For an introduction to “single-electronics,” see M. A. Kastner, *Rev. Mod. Phys.* **64**, 849 (1992); D. V. Averin and K. K. Likharev, in *Mesoscopic Phenomena in Solids*, edited by B. Altshuler *et al.* (North-Holland, Amsterdam, 1991); and several articles in *Single Charge Tunneling*, Vol. 294 of *NATO Advanced Study Institute, Series B: Physics* edited by H. Grabert and M. H. Devoret (Plenum, New York, 1992).
- ²F. R. Waugh, M. J. Berry, D. J. Mar, R. M. Westervelt, K. L. Campman, and A. C. Gossard, *Phys. Rev. Lett.* **75**, 705 (1995); see also F. R. Waugh, M. J. Berry, C. H. Crouch, C. Livermore, D. J. Mar, R. M. Westervelt, K. L. Campman, and A. C. Gossard, *Phys. Rev. B* **53**, 1413 (1996); F. R. Waugh, Ph.D. thesis, Harvard University, 1994.
- ³L. W. Molenkamp, Karsten Flensberg, and M. Kemerink, *Phys. Rev. Lett.* **75**, 4282 (1995).
- ⁴I. M. Ruzin, V. Chandrasekhar, E. I. Levin, and L. I. Glazman, *Phys. Rev. B* **45**, 13 469 (1992); L. I. Glazman and V. Chandrasekhar, *Europhys. Lett.* **19**, 623 (1992).
- ⁵C. A. Stafford and S. Das Sarma, *Phys. Rev. Lett.* **72**, 3590 (1994).
- ⁶C. A. Stafford and S. Das Sarma (unpublished).
- ⁷G. Klimeck, Guanlong Chen, and S. Datta, *Phys. Rev. B* **50**, 2316 (1994); Guanlong Chen, G. Klimeck, S. Datta, Guanha Chen, and W. A. Goddard III, *ibid.* **50**, 8035 (1994).
- ⁸D. S. Golubev and A. D. Zaikin, *Phys. Rev. B* **50**, 8736 (1994).
- ⁹S. V. Panyukov and A. D. Zaikin, *Phys. Rev. Lett.* **67**, 3168 (1991); *Phys. Lett. A* **183**, 115 (1993).
- ¹⁰A. D. Zaikin, D. S. Golubev, and S. V. Panyukov, *Physica B* **203**, 417 (1994).
- ¹¹G. Falci, J. Heins, Gerd Schön, and Gergely T. Zimanyi, *Physica B* **203**, 409 (1994); G. Falci, Gerd Schön, and Gergely T. Zimanyi, *Phys. Rev. Lett.* **74**, 3257 (1995).
- ¹²Herbert Schoeller and Gerd Schön, *Phys. Rev. B* **50**, 18 436 (1994).
- ¹³Hermann Grabert, *Phys. Rev. B* **50**, 17 364 (1994).
- ¹⁴L. I. Glazman and K. A. Matveev, *Zh. Éksp. Teor. Fiz.* **98**, 1834 (1990) [*Sov. Phys. JETP* **71**, 1031 (1990)]; K. A. Matveev, *ibid.* **99**, 1598 (1991) [**72**, 892 (1991)].
- ¹⁵H. O. Frota and Karsten Flensberg, *Phys. Rev. B* **46**, 15 207 (1992).
- ¹⁶Karsten Flensberg, *Physica B* **203**, 432 (1994); *Phys. Rev. B* **48**, 11 156 (1993).
- ¹⁷K. A. Matveev, *Phys. Rev. B* **51**, 1743 (1995).
- ¹⁸R. I. Shekhter, *Zh. Éksp. Teor. Fiz.* **63**, 1410 (1972) [*Sov. Phys. JETP* **36**, 747 (1973)]; I. O. Kulik and R. I. Shekhter, *ibid.* **68**, 623 (1975) [**41**, 308 (1975)].
- ¹⁹D. V. Averin and K. K. Likharev, *Zh. Éksp. Teor. Fiz.* **90**, 733 (1986) [*Sov. Phys. JETP* **63**, 427 (1986)]; *J. Low Temp. Phys.* **62**, 345 (1986).
- ²⁰In the experiment of Waugh *et al.* (Ref. 2) a channel between the dots is opened when the voltage on the gate tips framing the channel is changed by a relatively small percent. As the separation between the gate tips is approximately 100 nm, the above suggests that the potential landscape created by the applied voltages varies substantially over distances on the order of 50 nm that are approximately equal to a Fermi wavelength (40 nm).
- ²¹C. H. Crouch and J. M. Golden (unpublished).
- ²²For accounts of the formal theory of scattering, see, for example, Paul Roman, *Advanced Quantum Theory* (Addison-Wesley, Reading, MA, 1965) or Michael D. Scadron, *Advanced Quantum Theory* (Springer-Verlag, Berlin, 1991).
- ²³Matveev’s result in Ref. 17 arises from exponentiating $\ln(\pi W/N_{\text{ch}}e^\gamma U_2)$, where W is the Luttinger liquid’s ultraviolet cutoff. Luttinger-liquid theory’s unreliability in calculating the constant factors in the arguments of such logarithms is well documented. See, for example, J. Solyom, *Adv. Phys.* **28**, 201 (1979).
- ²⁴D. V. Averin and Yu V. Nazarov, in *Single Charge Tunneling* (Ref. 1), p. 217.
- ²⁵C. H. Crouch, C. Livermore, F. R. Waugh, R. M. Westervelt, K. L. Campman, and A. C. Gossard, *Proceedings of Electronic Properties of Two-Dimensional Systems XI* [*Surf. Sci.* (to be published)].
- ²⁶K. A. Matveev, L. I. Glazman, and H. U. Baranger, *Phys. Rev. B* **53**, 1034 (1996).